

Structural feature based collaborative reconstruction for quantitative susceptibility mapping

Lijun Bao^{1,2}, Zhong Chen¹, Peter C.M. van Zijl², and Xu Li²

¹Department of Electronic Science, Xiamen University, Xiamen, Fujian, China, ²Department of Radiology, School of medicine, Johns Hopkins University, Baltimore, MD, United States

Purpose Quantitative susceptibility mapping (QSM) enables non-invasive mapping and quantitative analysis of tissue magnetic susceptibility. However, the reconstruction of magnetic susceptibility distributions from local phase information is an ill-posed inverse problem. The calculation of susceptibilities through multiple orientation sampling (COSMOS)¹ provides high quality images, but acquiring such data is inconvenient especially for in vivo study of patients. According to the observation that the morphology information extracted from the acquired magnitude image shares common features with that extracted from susceptibility maps, regularization methods based on a priori information extracted from magnitude data, such as morphology enabled dipole inversion (MEDI), have been proposed^{2,3,4}. However, there are still some tissue edges that can be easily observed in susceptibility maps but have little or no contrast in magnitude images (arrows in Fig. 1(c)-(d)), which generates possible errors for MEDI. We propose a structural feature based collaborative reconstruction (SFCR) method for QSM to address this issue.

Theory Denoting the dipole kernel in the k-space with $C_k(k) = (1/3 - k_z^2/k^2)$, the susceptibility map can be obtained as $\chi_k(k) = C_k(k)^{-1} \varphi_k(k)$, where χ is the susceptibility distribution and φ is the measured field map. Our proposed approach is composed of two steps: the M-step and S-step.

A. M-step: regional adaptive reconstruction based on magnitude a priori

First, we reconstruct the susceptibility map $\hat{\chi}$ by employing a regional adaptive model based on compressed sensing as

$$\hat{\chi} = \arg \min \lambda_1 \|\chi(k)H - \text{diag}(H)F\chi\|_2^2 + \|\mathbf{P}_{\text{mag}} \nabla \chi\|_1 + \lambda_2 \|\mathbf{R}\chi\|_2 \quad (1)$$

where F is a Fourier operator to transform χ into Fourier transform domain. H is a binary mask corresponding to the well-conditioned and ill-conditioned subdomains. The weighting matrix \mathbf{P}_{mag} is set as a binary mask assigned zero to the voxels with large magnitude gradients ∇M and one to those voxels with small gradients. ∇ denotes the three dimensional gradient operator. The last item is a smooth constraint with a ROI mask. λ_1 and λ_2 are regularization parameters.

B. S-step: collaborative reconstruction based on susceptibility structural feature

To compensate the differences in the a priori derived from susceptibility and that from magnitude image, we propose to use the susceptibility $\hat{\chi}$ obtained in the M-step to formulate collaborative reconstruction model with

$$\chi = \arg \min \gamma_1 \|\Phi(C\chi - \varphi)\|_2^2 + \|\mathbf{P}_\chi \nabla \chi\|_1 + \gamma_2 \|\mathbf{R}\chi\|_2^2 \quad (2)$$

The fidelity term in S-step is evaluated in the spatial domain as a complementary to the M-step fidelity term in k-space. Φ is a weighting matrix proportional to SNR of each voxel. With a weighted $l1$ sparse constraint, textures and edges corresponding to the structural features in the susceptibility distribution are emphasized in the reconstruction, while tiny variations are suppressed as noise. The feature weighting matrix \mathbf{P}_χ is derived from the susceptibility gradients of $\hat{\chi}$ with threshold μ_{sus} . The objective functions are two convex optimization problems. By introducing a variable $\mathbf{b} = \|\mathbf{P}\nabla\chi\|_1$, it can be solved in two sub-procedures: fixed χ and solving \mathbf{b} by iterative threshold shrinkage algorithm, and then fixed \mathbf{b} to solve χ with conjugate gradient algorithm.

Methods In vivo healthy human brain data were acquired at 7T Philips Health-care using a 32-channel Novamedical head coil. A 3D multi-echo GRE sequence was used with 1 mm isotropic resolution, matrix size of $224 \times 224 \times 110$, TR/TE1/ΔTE=45/2/2ms, 16 echoes⁵. Each subject was scanned with the head placed at four different orientations. COSMOS was calculated using data from all four directions and used as gold standard. In addition, QSMs for a single orientation were calculated using TDK⁶, LSQR⁵, MEDI⁴ and SFCR. Parameters in SFCR were set as $\lambda_1=50$, $\lambda_2=1$, $\gamma_1=6000$, $\gamma_2=30$, while λ in MEDI⁴ was optimized to 10,000. A ROI based quantitative comparison was performed, in which susceptibility values were measured relative to CSF in lateral ventricles. ROIs were selected based on a human brain atlas⁵.

Results and Discussion As shown in Fig.1, tissue edges derived from magnitude images (c) and susceptibility maps (d) have some quality differences (indicated by arrows). Using COSMOS as a reference, we found that susceptibility maps generated by SFCR presented better structure consistency (red circles) and better artifact suppression than other single orientation QSM methods, especially in the regions with susceptibility changing sharply (white arrows). Susceptibility values calculated by different methods in selected deep gray matters are shown in Fig.2. The SFCR reconstruction accuracy is evaluated in Table 1 using the fidelity error $\|\mathbf{C}\chi - \varphi\|_2^2$, QSM RMSE, structure similarity MSSIM to COSMOS, and computation time. Compared to MEDI, SFCR achieved less fidelity error and RMSE, higher structure agreement and reduced computation time.

Conclusion The proposed SFCR method utilizes collaborative reconstruction compensating the structure differences in susceptibility and magnitude images to achieve more accurate QSM estimation. Combining iterative threshold shrinkage algorithm with conjugate gradient algorithm can further facilitate optimization problem solution. These may help the QSM technology to get a wider range of applications.

Acknowledgment This work was supported by NNSF of China under Grants 81301277, Research Fund for the Doctoral Program of Higher Education of China under Grant 20130121120010 and NSF of Fujian Province of China under Grant 2014J05099, and by NIH grant P41 EB015909.

References 1. Liu T, et al. Magn Reson Med, 2009. 2. Wu B, et al. Magn Reson Med, 2012. 3. Schweser F, et al. NeuroImage, 2012. 4. Liu T, et al. Magn Reson Med, 2013. 5. Li X, et al. NeuroImage, 2012. 6. Wharton S, et al. Magn Reson Med, 2010.

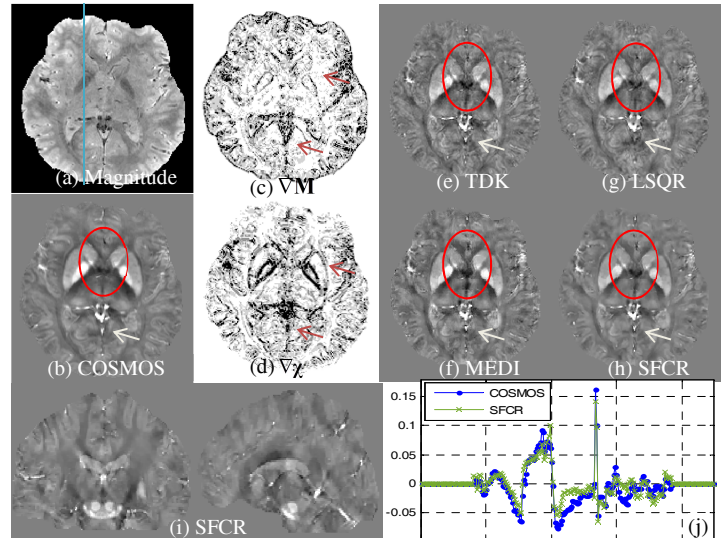


Fig.1 In vivo human brain data at 7T. (a) the magnitude image, (b) QSM using COSMOS, (c) and (d) are gradient maps of (a) and (c); (e)-(h) are calculated QSMs with TDK, LSQR, MEDI and SFCR shown in scale [-0.15,0.15]ppm. (i) coronal and sagittal view of SFCR, (j) QSM profile along the line drawn on (a).

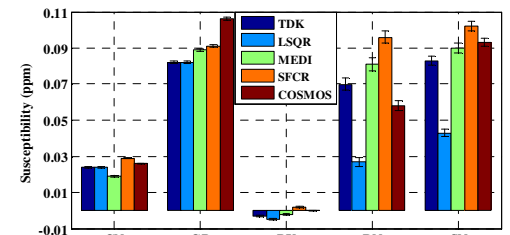


Fig.2 Susceptibility comparison (mean \pm standard error) in different brain regions. CN: caudate nucleus, GP: globus pallidus, PU: putamen, RN: red nucleus, SN: substantia nigra.

Table 1 SFCR reconstruction performance evaluation.

Method	Error	RMSE	MSSIM	CompTime/s
TDK	1.83	29.94	0.9354	0.25
LSQR	27.28	23.40	0.9666	1427.35
MEDI	12.43	23.75	0.9664	146.18
SFCR	10.33	18.52	0.9776	124.88